

Article

The Effect of Sodium Alginate on Chlorite and Serpentine in Chalcopyrite Flotation

Guangjiu Pan ¹, Guofan Zhang ^{1,2}, Qing Shi ^{1,2,*} and Wei Chen ³

¹ School of Minerals Processing and Bioengineering, Central South University, Changsha 410083, China; panguangjiu@csu.edu.cn (G.P.); zhangguofan@csu01@126.com (G.Z.)

² Key Laboratory of Hunan Province for Clean and Efficient Utilization of Strategic Calcium-Containing Mineral Resources, Central South University, Changsha 410083, China

³ College of Materials and Mineral Resources, Xi'an University of Architecture and Technology, Xi'an 710055, China; xauatchchenwei@163.com

* Correspondence: shiqok@csu.edu.cn; Tel.: +86-731-8883-0913

Received: 23 February 2019; Accepted: 22 March 2019; Published: 26 March 2019



Abstract: Chlorite and serpentine are common magnesium-containing gangue minerals in copper sulfide flotation. In this study, sodium alginate, a natural hydrophilic polysaccharide, was introduced as a selective depressant for these gangue minerals. Micro-flotation tests were conducted on both single minerals and synthetic mixtures. The flotation results showed that sodium alginate could simultaneously depress the flotation of chlorite and serpentine effectively, but seldom influenced the floatability of chalcopyrite at pH 9. In the ternary mixture flotation, a concentrate with a Cu grade of 31% could be achieved at Cu recovery of 90%. The selective depression of chlorite and serpentine was also validated by the real ore flotation experiments. The selective depression mechanism was investigated through adsorption tests, zeta potential measurements, and FTIR analyses. The adsorption density results implied that sodium alginate selectively adsorbed on the surface of phyllosilicates, but no adsorption on the chalcopyrite surface was observed. The zeta potential results showed that the sodium alginate could selectively decrease the surface charge of chlorite and serpentine. The FTIR results revealed the chemical adsorption of sodium alginate on the chlorite and serpentine surface and no form of adsorption on chalcopyrite, agreeing well with the adsorption density results. On the basis of these results, a selective adsorption model of sodium alginate on the mineral surface was proposed.

Keywords: flotation; sodium alginate; depressant; chlorite; serpentine

1. Introduction

Chlorite and serpentine are typical magnesium-rich phyllosilicates in copper sulfide deposits [1,2]. Generally, chlorite is the secondary alteration product of rich magnesium-iron silicate minerals in magma [3], and serpentine is the metasomatic reaction product of hydrothermal fluid to olivine in ultrabasic rocks [4]. Since serpentinization is often accompanied by chloritization [5,6] and both phyllosilicates are products of hydrothermal alteration, they often appear together in the same deposits [7]. At present, flotation is the most commonly-used method to separate the valuable copper sulfide mineral from these two phyllosilicates. Nevertheless, due to the unique properties of chlorite and serpentine, the phyllosilicates impair the flotation of copper sulfide ore. A high content of these phyllosilicates in slurry increases the pulp viscosity [8,9], which can result in a significant reduction in flotation recovery [10]. These phyllosilicates also adhere to valuable minerals to form a hydrophilic coating, which prevents the adsorption of collectors on sulfide minerals and reduces their floatability [11]. In addition, the high entrainment of phyllosilicates significantly reduces the

grade of flotation concentrates, and high levels of the MgO silicates in concentrates cause problems in downstream processing, such as increasing smelting costs and reducing recovery [12]. Therefore, the depression of phyllosilicates in the flotation of copper sulfide has received much attention.

However, these two phyllosilicates have different crystal structures and surface properties and further affect flotation in different ways. Chlorite is a 2:1 phyllosilicate with an interlayer brucite-like sheet containing Mg, Al, and Fe octahedrally coordinated [13]. After the liberation, there are broken bonds of the brucite-like sheet, which cause staggered charged surfaces. It is easy for anionic and cationic collectors to adsorb on the staggered broken sides so that chlorite is naturally floatable [14]. Entrainment is considered to be another way of chlorite deteriorating flotation. Cu^{2+} in solution can also activate the flotation of chlorite [15], which makes the situation even worse. Different from chlorite, serpentine has a 1:1 layer structure. When serpentine dissociates, the magnesia octahedral layer breaks, and there are many Mg–O bonds exposed on the surface. Due to the transfer of –OH from the serpentine surface to the slurry in preference to Mg^{2+} , the surface of the serpentine is positively charged [16,17]. In the pH range commonly used in flotation, the surface charges of the serpentine and valuable mineral are generally opposite, and this contrast leads to flotation deterioration by hetero-aggregation or slime coating, which decreases the floatability of the sulfide particles [18,19].

Since the influencing mechanisms of chlorite and serpentine are dissimilar, their flotation depression methods are different. The depression of chlorite is achieved by increasing its surface hydrophilic ability, thus reducing its floatability. The depressants primarily include sodium silicate, hydrogen fluoride, tripolyphosphate, and a variety of other polysaccharides [13]. For serpentine, however, the depression is principally achieved by creating electrical repulsion or steric hindrance to disperse serpentine from valuable particles' surfaces. In order to disperse serpentine particles, sodium hexametaphosphate, sodium carbonate, and other organic agents are used [20]. Large molecular depressants are commonly-used reagents to depress phyllosilicates. Polysaccharides, such as carboxymethyl cellulose (CMC) [21], chitosan [22], guar gum [23], dextrin [24], and lignosulfonate [25], have been applied to eliminate the harmful effects of phyllosilicates. The most reported polymeric depressant is carboxymethyl cellulose (CMC), which has been widely used for depressing MgO-type gangue minerals in nickel sulfide flotation [10]. Although many works on the polysaccharide depressants of chlorite and serpentine have been presented, they have generally focused on the condition that one kind of magnesium silicate-bearing gangue mineral is present in the ores.

Sodium alginate (NaAl), generally derived from kelp or Sargassum, is a natural hydrophilic polysaccharide with a backbone of (1-4)-linked β -D-mannuronic acid (M units) and α -L-guluronic acid (G units). It can form irregular patterns of GG, MG, and MM blocks [26,27] (Figure 1). With characteristics of high stability, non-toxicity, and excellent biocompatibility, NaAl has an extensive use as a heavy-metal binder, thickener, stabilizer, and drug-controlled release matrix [28–30]. As plenty of chelating groups, such as hydroxy (–OH) and carboxyl (–COO–), are distributed along the backbone, NaAl can interact with metallic ions on the mineral surfaces [31–34]. The chelating ability of –OH and –COO– in NaAl with Ca^{2+} has been successfully applied to separate scheelite from calcite and fluorite [35]. Besides, researchers have found that NaAl could chemically adsorb on the molybdenite surface through –OH and –COO–, but had little effect on chalcopyrite flotation [36]. Therefore, it is possible for NaAl to adsorb on the phyllosilicate surface selectively. The adsorption of NaAl on the mineral surface makes phyllosilicates surfaces more hydrophilic in solution and generates strong surface electrical repulsion and steric hindrance effects. Although a handful of papers referring to employing NaAl as a depressant have been published [35,36], there are no references on the application of NaAl to depress chlorite and serpentine simultaneously.

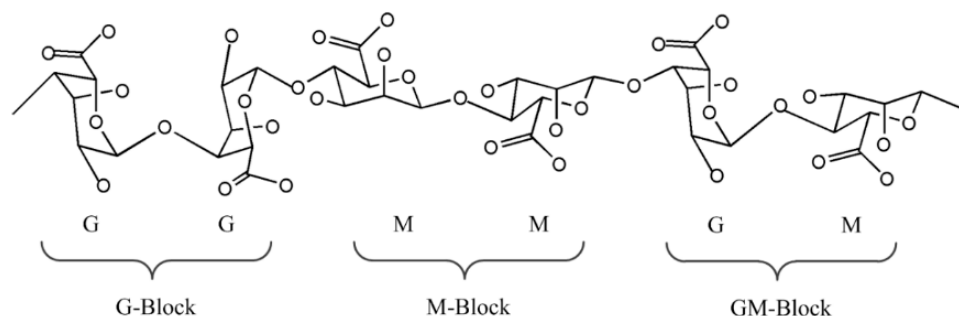


Figure 1. Structure of sodium alginate [27].

This study is aimed at introducing sodium alginate (NaAl) as an effective depressant to simultaneously depress chlorite and serpentine in copper sulfide flotation. Chalcopyrite was chosen to be a representative of copper sulfide minerals. Micro-flotation tests of single mineral and synthetic mixtures were carried out to show the effective inhibition effect of NaAl on both chlorite and serpentine. The real ore flotation experiments were also conducted to show the selective depression of NaAl on chlorite and serpentine. The depression mechanism of NaAl was investigated by adsorption tests, zeta potential measurements, and Fourier transform infrared (FTIR) spectra, by which a possible adsorption model was put forward.

2. Material and Methods

2.1. Pure Minerals and Reagents

Chalcopyrite, chlorite (clinochlore), and serpentine (lizardite) samples used in this study were purchased from Yip's Mineral Specimen Factory (Guangzhou, China). X-ray fluorescence (XRF) analysis and X-ray diffraction (XRD) results of three mineral samples are given in Table 1 and Figure 2, respectively. The XRD results were analyzed with the RIR (Reference Intensity Ratio) value method for phase semi-quantitative analysis. The analysis showed that the purities of the mineral samples were 97.19% (for chalcopyrite), 98.82% (for chlorite), and 90.88% (for serpentine). Since the samples were all of the high purity (above 90%), no further cleaning was necessary. The pure mineral samples were first hammered into small pieces and then ground in a ceramic ball mill. The ground samples were dry-sieved to obtain $-75 + 38 \mu\text{m}$ -size fractions for the micro-flotation tests. Next, the samples below $-38 \mu\text{m}$ were further ground to $-10 \mu\text{m}$ (by Sichuan Dewei Weina Technology Co., Ltd., using jet milling, Mianyang, China) for the adsorption tests, zeta potential measurements, and FTIR studies.

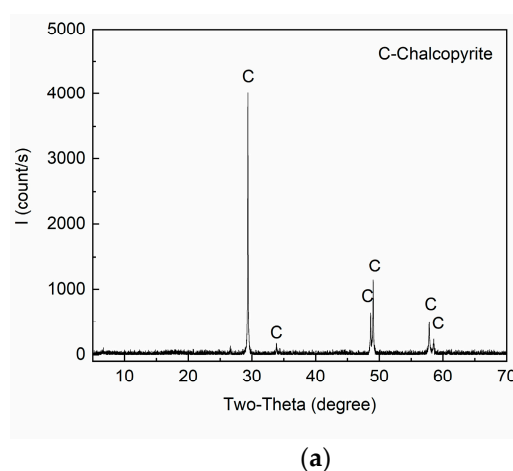
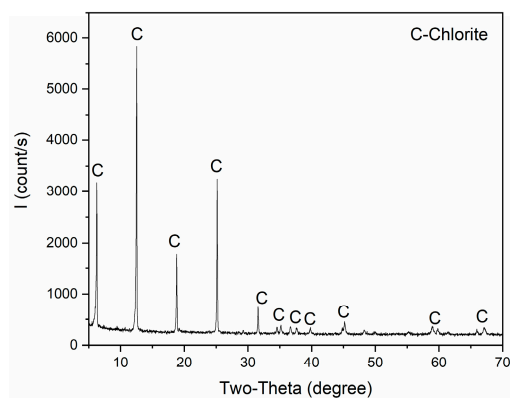
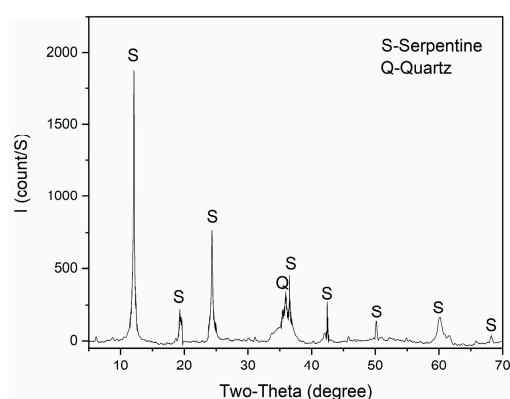


Figure 2. Cont.



(b)



(c)

Figure 2. XRD spectra of the chalcopyrite (a), chlorite (b), and serpentine (c) samples**Table 1.** Chemical compositions of chalcopyrite, chlorite, and serpentine.

Elements	Cu	Fe	S	MgO	SiO ₂	Al ₂ O ₃	CaO	Others
Chalcopyrite	33.88	29.45	33.86	/	2.81	/	/	/
Chlorite	/	31.69	/	15.41	41.10	11.32	0.28	0.20
Serpentine	/	1.08	/	38.92	46.13	1.16	0.61	12.10

Sodium amyl xanthate (SAX) and methyl isobutyl carbinol (MIBC), obtained from Tianzhuo Flotation Reagent Co., Ltd. (Ganzhou, China), were used as a collector and a frother, respectively. NaAl was purchased from Tianjin Guangfu Fine chemical Research Institute with a molecular mass of approximately 50,000 and employed as a depressant. pH adjustment was achieved by the addition of hydrochloric acid (HCl) and sodium hydroxide (NaOH). Distilled water was used in all of the experiments.

2.2. Experiments

2.2.1. Micro-Flotation Experiments

The single mineral flotation tests were conducted in an XFGC mechanical agitation flotation machine at 1992 rpm with a 40-mL cell. For single mineral flotation, 2 g of pure mineral was added into the flotation cell with 40 mL of distilled water. The pH was adjusted to the desired value (2, 4, 6, 8, 10, and 12) using NaOH or HCl within 3 min. Then, the pulp was continuously stirred for 3 min with the depressant (if needed), 3 min with the collector (20 mg/L), and 2 min with the frother (20 mg/L). After 4 min of flotation, the flotation products (both the float and sink particles) were collected, filtered,

dried, and weighed. The flotation recovery was calculated based on solid weight distributions between two flotation products.

For synthetic mixture flotation, the mass ratios of chalcopyrite and gangue mineral were 1:1 for the binary mixtures (1 g chalcopyrite + 1 g chlorite or serpentine) and 4:3:3 for the ternary mixture (0.8 g chalcopyrite + 0.6 g chlorite + 0.6 g serpentine). In the following text, the mixture of chalcopyrite and chlorite was referred to as the binary mixture 1, while that of chalcopyrite and serpentine was referred to as the binary mixture 2. The flotation procedure used for mixtures was identical to that used for single mineral flotation. After the flotation experiments, the concentrates and tailings were collected and analyzed for Cu grade. The recovery was calculated by Cu distributions between two flotation products. The Cu grade was 16.9% for original binary mixtures and 13.6% for original ternary mixtures.

2.2.2. Batch Flotation Tests

The batch flotation tests were conducted in a 1.5-L XFD-IV single-trough flotation machine (made by Jilin Exploration Machinery Factory, Changchun, China). The real ore containing 1.3% Cu was supplied by Jinchuan Group Ltd. (Jinchang, China). For each test, 500 g of raw ore was wet ground to 75 wt % passing 75 μm with a ball mill. The slurry was transferred into the flotation cell and stirred for 3 min. The sodium hexametaphosphate (200 g/t) and NaAl were added sequentially and conditioned for 3 min of each. Then, sodium amyl xanthate (120 g/t) and ammonium butyl aerofloat (60 g/t) were added together and stirred for 3 min. After the 12-min single-stage rougher flotation, the rougher concentrate and tailing products were filtered, dried, weighed, sampled, and assayed for Cu. Tap water and industrial-grade reagents were used in all batch flotation experiments. The flow sheet and conditions of flotation tests are demonstrated in Figure 3.

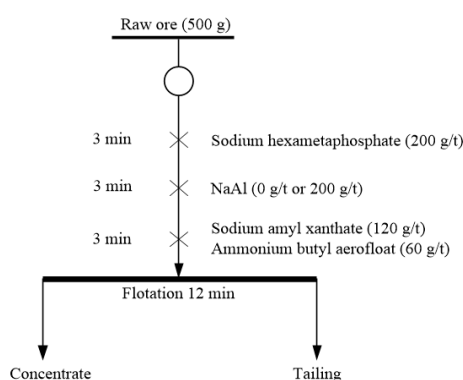


Figure 3. The beneficiation flow sheet of real ore experiments.

2.2.3. Adsorption Tests

In this study, the NaAl adsorption density on mineral particle surface was calculated by the residual concentration method. The reagent concentration was tested with a TOC-L machine from Shimadzu, Kyoto, Japan, and the value compared to a known calibration standard. The calibration standard was obtained by fitting the total organic carbon with the concentration (0, 5, 10, 20, 30, 40, 50, 60, 80, 120, 200) of pure NaAl solution at pH 9. For each adsorption test, 2 g of $-10 \mu\text{m}$ mineral (single mineral) was added into an 80-mL beaker together with 40 mL of NaAl solution, which was prepared at the desired concentration (5, 10, 20, 30, 40, 50, 60, 80, 120 mg/L) at pH 9. The suspension was stirred for 40 min using a magnetic stirrer and then centrifuged. The concentration of NaAl left in the supernatant was measured using the total organic carbon (TOC) by the TOC-L machine (Shimadzu, Kyoto, Japan) and the value compared to the known calibration standard. It was assumed that the amount of NaAl depleted from solution had adsorbed onto the minerals' surfaces. The unit of adsorption amount obtained using TOC was mg/L. In order to compare the adsorption capacity between different samples, the unit of adsorption capacity was converted from mg/L to mg/m^2 . Namely, the adsorption amount obtained using TOC was divided by the product of the sample mass

per unit volume and the specific surface area of the sample. The specific surface area of three minerals was measured with an automatic specific surface analyzer (Monosorb, Quantachrome Corp, Boynton Beach, FL, USA). The surface areas of chalcopyrite, chlorite, and serpentine were 11.64, 14.58, and 12.29 m²/g, respectively.

2.2.4. Zeta Potential Measurements

Zeta potential measurements on chlorite, serpentine, and chalcopyrite were conducted using a Coulter Delsa 440sx Zeta analyzer instrument (Beckman Coulter, Brea, CA, USA). The zeta potentials of three minerals in the absence and presence of NaAl were tested. In the zeta potential measurements of minerals in the presence of NaAl, 30 mg of the −10 μm-size fraction mineral was dispersed in 40 mL of the KNO₃ solution (1 × 10^{−3} mol/L). Pulp pH was adjusted to 2, 4, 6, 8, 10, and 12 with HCl or NaOH within 10 min. Then, the depressant (80 mg/L NaAl) was added for 10 min conditioning under room temperature (25 °C). After standing for 5 min, the suspension was used for the zeta potential measurement. The zeta potential measurement of the minerals in the absence of NaAl was identical to the procedure of the measurement in the presence of NaAl, except for no addition of NaAl after adjusting the pH. To keep the stirring time consistent with the condition in the presence of NaAl, the suspension was also conditioned for 10 min before standing for 5 min.

2.2.5. FT-IR Studies

For the FTIR studies, 0.5 g of the −10 μm mineral sample was conditioned with flotation reagents in 30 mL of aqueous solution at pH 9 for 40 min. After conditioning, the suspension was centrifuged. The precipitate was washed three times with distilled water and then vacuum dried at 40 °C. The spectroscopy measurement was carried out with a Spectrum One FT-IR (Version BM, PerkinElmer, Waltham, MA, USA) spectrometer using the diffuse reflection method, and the spectra were recorded with 30 scans at a resolution of 2 cm^{−1}.

3. Results and Discussion

3.1. Micro-Flotation Experiments

The effect of pulp pH and NaAl dosages on the flotation recovery of chalcopyrite, chlorite, and serpentine were tested, and the results are shown in Figures 4 and 5.

Figure 4a shows the flotation behaviors of single minerals at different pH in the absence of NaAl. Chalcopyrite and chlorite were floatable with recoveries of around 92% and 55%, respectively; and their floatability was barely affected by the change of pH. The recovery of serpentine was very low (less than 40%), especially under strong acid condition. Although the flotation recovery of chalcopyrite was much higher than that of chlorite and serpentine in the pH range of 2–12, a good flotation separation was still difficult to achieve because the naturally-floatable chlorite would get into the concentrate, and serpentine would impair chalcopyrite flotation.

The effect of pH on the flotation performance of synthetic mixtures is shown in Figure 4b. According to Figure 4b, pH had a negligible effect on the separation of chalcopyrite from phyllosilicates. For the binary mixture 1, pH had little effect on the separation of chalcopyrite from chlorite. The Cu grade in all concentrates was only a bit higher than that in the original mixture (Cu grade 16.9%), suggesting that many naturally-floatable chlorite particles were in the concentrates, and therefore reducing the concentrate grade. For the binary mixture 2, serpentine impaired the flotation by reducing the Cu recovery [37]. It is known that serpentine particles adhere to the sulfide particles in hetero-aggregation or slime coating, which decreases the floatability of the sulfide particles. In Figure 4b, the Cu recovery of the binary mixture 2 was lower than 71% in the tested pH range of 2–12, much less than that of single chalcopyrite flotation (all above 90%). In the binary mixture systems, the influence of phyllosilicates was straight forward because chlorite only affected Cu grade and serpentine impaired Cu recovery.

However, in the ternary mixture system, the influence became much more complex. It was observed that both Cu recovery and grade dramatically decreased in the entire pH range. The Cu recovery of the ternary mixture decreased to less than 70% from 90% (the recovery of single chalcopyrite flotation). The Cu grade also decreased to less than 22%. The ternary mixture flotation results indicated that the detrimental effect of chlorite and serpentine was superimposed in chalcopyrite flotation, and the depression of phyllosilicates was more difficult in the ternary system than that in the binary systems. Since chlorite and serpentine were oppositely charged, they may attracted each other through an electrostatic mechanism. In the ternary mixture system, serpentine adhered to both chalcopyrite and chlorite, which decreased the floatability of chalcopyrite and impaired the depression of chlorite.

According to Figure 4, the two phyllosilicates impaired chalcopyrite flotation in different ways, and a good flotation separation was difficult to achieve by adjusting pH in the absence of depressant, especially in the ternary mixture system.

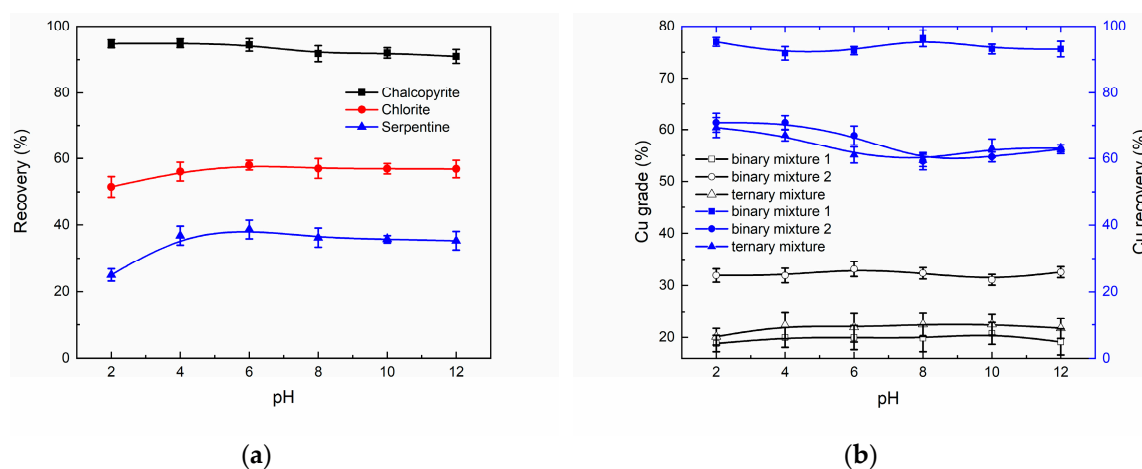


Figure 4. Effect of pH on the flotation behavior of single minerals (a) and mixed minerals (b). [sodium amyl xanthate (SAX)] = 20 mg/L; [methyl isobutyl carbinol (MIBC)] = 20 mg/L; binary mixture 1: the mixture of chalcopyrite and chlorite; binary mixture 2: the mixture of chalcopyrite and serpentine.

Since pH 9 was chosen in reported studies and industrial applications as conventional flotation conditions [38–40], the pH of the following experiments was also set as 9. The effect of NaAl dosages on the flotation performance of single minerals at pH 9 is shown in Figure 5a. It was observed that NaAl showed a potent inhibitory effect on both chlorite and serpentine, but rarely affected the floatability of chalcopyrite. As the NaAl dosage increased to 40 mg/L, the recoveries of chlorite and serpentine simultaneously decreased to less than 5% from their initial values (60% and 36%, respectively), whereas the recovery of chalcopyrite remained at a high level (above 90%). The flotation results implied that NaAl could be employed as an effective depressant to separate chalcopyrite from chlorite and serpentine at pH 9.

Based on the single mineral flotation results, synthetic mixtures flotation tests were carried out to validate the selective depression effect of NaAl at pH 9. The results obtained are shown in Figure 5b. For the binary mixture 1, the Cu grade gained a significant improvement after the addition of NaAl. For the binary mixture 2, the addition of NaAl improved Cu recovery. The binary mixture flotation results confirmed that NaAl had an excellent selectivity of depression. In the ternary mixture system, significant improvements in both Cu recovery and grade were observed. Without adding NaAl, the Cu grade was only 22%; whereas a concentrate with a Cu grade of 31% could be achieved when the dosages of NaAl increased to 40 mg/L. Similarly, as the dosages of NaAl increased to 40 mg/L from 0 mg/L, the Cu recovery increased to 91% from 62%. The ternary mixture flotation results indicated that NaAl simultaneously depressed chlorite and serpentine. According to Figure 5b, with a further increase on the dosage of NaAl (up to 120 mg/L), no further improvement on flotation was observed

as the maximum Cu recovery and grade were already reached, indicating that that 40 mg/L would be sufficient for the flotation separation for binary and ternary mixtures.

The single mineral and synthetic mixture flotation results showed that it was feasible to utilize NaAl as a depressant to depress chlorite and serpentine simultaneously.

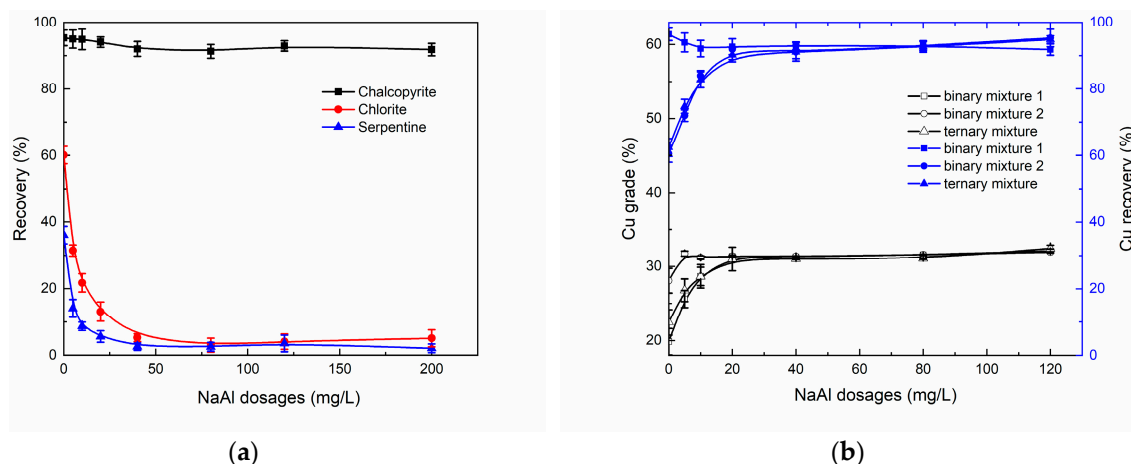


Figure 5. Effect of NaAl dosages on the flotation behavior of single minerals (a) and mixed minerals (b). [SAX] = 20 mg/L; [MIBC] = 20 mg/L; pH = 9.

3.2. Real Ore Flotation Experiments

To validate the effect of NaAl on flotation separation of chalcopyrite from chlorite and serpentine, real ore flotation experiments were conducted. A feed material containing 1.3% Cu from Jinchuan Group Ltd. was used for the rougher flotation of chalcopyrite in this study. Table 2 shows the effect of NaAl on the flotation separation of real ore. It can be seen that the addition of NaAl increased the Cu grade from 2.6% to 3.2% and the Cu recovery from 65.5% to 73.2%. The real ore outcomes indicated that NaAl could be used in industrial applications in the flotation separation of chalcopyrite from chlorite and serpentine.

Table 2. Effect of NaAl on the flotation separation of real ore.

Conditions	Product	Yield (%)	Cu Grade (%)	Cu Recovery (%)
NaAl 0 g/t	Concentrate	33.5	2.6	65.5
	Tailing	66.5	0.7	34.5
	Feed	100.0	1.3	100.0
NaAl 200 g/t	Concentrate	30.2	3.2	73.2
	Tailing	69.8	0.5	26.8
	Feed	100.0	1.3	100.00

3.3. Adsorption Experiments

Figure 6 shows the adsorption of NaAl on chalcopyrite, chlorite, and serpentine surfaces. The adsorption density of chlorite and serpentine increased with an increase of NaAl dosages in the range of 5–80 mg/L. When the addition dosage exceeded 80 mg/L, the adsorption on the surface of gangue minerals reached saturation with the adsorption density of 0.14 mg/m² for chlorite and 0.24 mg/m² for serpentine. Compared to the two gangue minerals, the adsorption density on the surface of chalcopyrite was negligible (less than 0.02 mg/m²). The results for the adsorption measurement indicated that NaAl selectively adsorbed on the surface of chlorite and serpentine and hence showed an inhibitory effect, which was in good agreement with the flotation results.

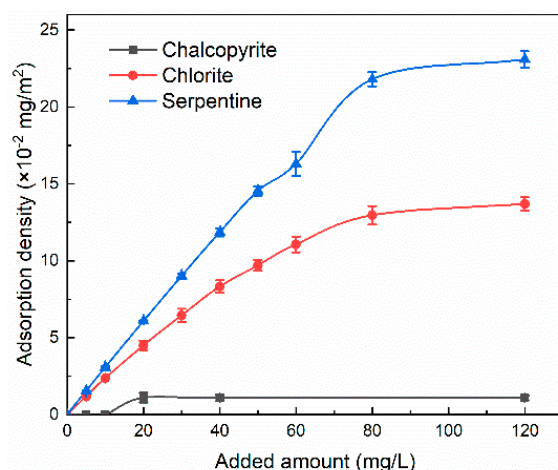


Figure 6. Adsorption density of NaAl on the minerals' surface as a function of concentration at pH = 9.

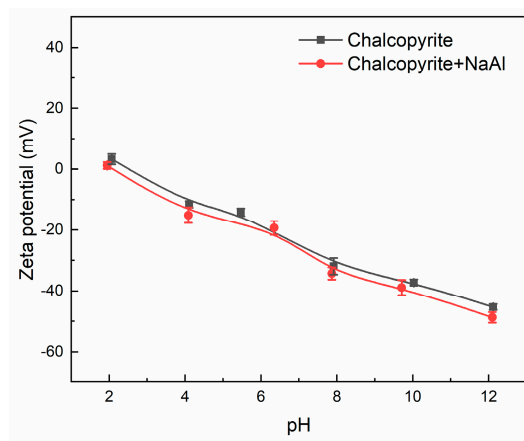
3.4. Zeta Potential Measurement Results

The zeta potentials of chalcopyrite, chlorite, and serpentine minerals in the absence and presence of NaAl were measured, and the results are shown in Figure 7.

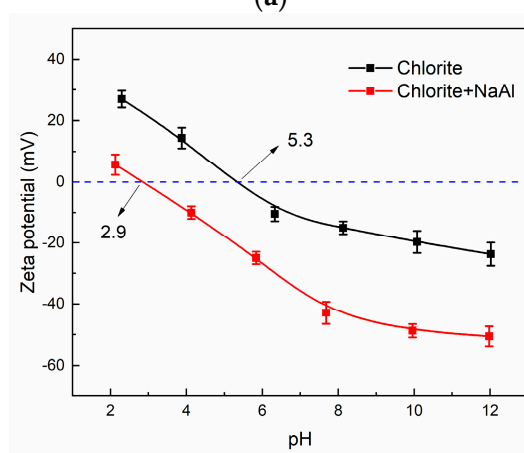
As can be seen in Figure 7a, the zeta potentials of chalcopyrite decreased from 3.2 mV to -45.4 mV in pH 2–12. After the interaction with NaAl, there was a small negative shift in the zeta potentials of chalcopyrite. The results implied that the NaAl showed no significant effect on the zeta potentials of chalcopyrite, and there was little NaAl adsorbed on the surface of chalcopyrite. Under pH 9, the zeta potential of chalcopyrite was -34.4 mV, and NaAl was also negatively charged in the solution, resulting in strong electrostatic repulsion between mineral and reagent. The electrostatic repulsion hindered the approach of NaAl to chalcopyrite and further weakened the interaction between the mineral and NaAl. Therefore, no depression effect on chalcopyrite was observed.

According to Figure 7b,c, the zeta potentials of chlorite and serpentine decreased in the pH range of 2–12. It could also be seen from Figure 7b,c that the addition of NaAl resulted in significant shifts on the iep (isoelectric point) of chlorite and serpentine, which moved from 5.3 to 2.9 and from 11.7 to 4.0, respectively. Since plenty of free hydroxyl and carboxyl groups along the backbone endowed NaAl with negative charges in solution [26], it was reasonable to infer that abundant adsorption of NaAl on the surfaces of phyllosilicates was responsible for these remarkable shifts. Different from chalcopyrite, the electrostatic repulsion between NaAl and chlorite was much smaller. It was much easier for NaAl to approach the surface of chlorite. The charges of NaAl and serpentine were opposite at pH 9. There was an electrostatic attraction between NaAl and serpentine, which facilitated the approach of NaAl to serpentine. After interacting with NaAl at pH 9, the zeta potential of chlorite experienced a shift of -29.0 mV (from -17.1 mV to -46.1 mV), and that of serpentine also experienced a shift of -40.5 mV (from 14.7 mV to -25.8 mV). As the zeta potential of serpentine had a larger change, there should be a greater amount of NaAl adsorbing on the serpentine surface, which was in line with the adsorption density results.

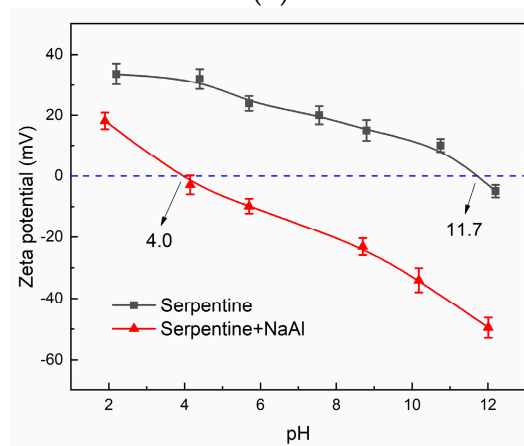
The zeta potential results of three minerals showed that NaAl could selectively change the zeta potential of chlorite and serpentine, indicating selective adsorption on the surfaces of two gangue minerals.



(a)



(b)



(c)

Figure 7. Effect of pH on the zeta potential of chalcopyrite (a), chlorite (b), and serpentine (c) in the absence and presence of NaAl. [NaAl] = 80 mg/L.

3.5. IR Spectroscopic Analysis

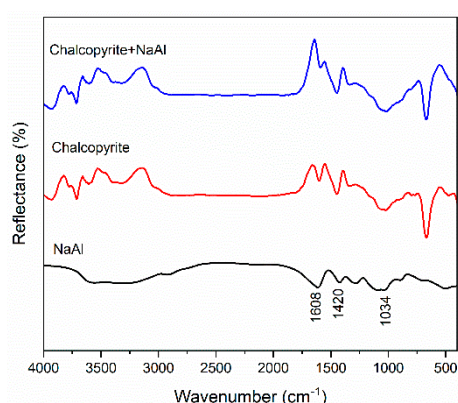
IR spectroscopy was performed to define the adsorption mechanism of NaAl on the surface of the three minerals. The IR spectra results can be seen in Figure 8.

In the IR spectrum of NaAl, the anti-symmetric stretching vibration of -COO- emerged at 1608 cm^{-1} , and the symmetrical stretching vibration appeared at 1420 cm^{-1} [41]. The characteristic peaks at 1034 cm^{-1} were considered to be the stretching vibration of C-O-C [42].

IR spectra of chalcopyrite with and without pre-treatment of NaAl are shown in Figure 8a. According to Figure 8a, it was clear that NaAl had a negligible effect on the spectrum of chalcopyrite. After conditioning with NaAl, there were no new characteristic adsorption bands observed, which implied that the adsorption ability of NaAl on chalcopyrite was fairly weak.

Figure 8b shows the IR spectra of chlorite with and without pre-treatment of NaAl. FTIR spectra of bare chlorite showed peaks at 3744 cm^{-1} , 3411 cm^{-1} , 1000 cm^{-1} , indicating the stretching of Si-OH , -OH , and Si-O , respectively. The bending vibration of -OH and Si-O appeared at 656 cm^{-1} and 472 cm^{-1} , respectively. After interacting with NaAl, adsorption bands at 1000 cm^{-1} experienced a change to 1027 cm^{-1} , and a broader and blunter peak form was observed, which was owing to the stretching vibration of C-O-C of NaAl at 1034 cm^{-1} . The results suggested the adsorption of NaAl on the surface of chlorite. It should be noted that the -OH stretching peak of silanol groups at 3744 cm^{-1} disappeared. The disappearance of stretching peaks of -OH suggested that silanol groups on the surface of chlorite interacted with carboxyl groups of NaAl [43]. The adsorption bands of -COO- in NaAl were also observed on the surface of chlorite. However, they had shifted from 1608 cm^{-1} and 1420 cm^{-1} to 1633 cm^{-1} and 1424 cm^{-1} , respectively, indicating that the adsorption of NaAl on chlorite surface was chemical in essence. Previous studies found that metal ions on the surfaces of chlorite complexed with carboxylate functional groups [44–46]. Therefore, it was reasonable to infer that the metal ions (Al^{3+} , Fe^{2+} , Mg^{2+}) on the surfaces of chlorite interacted with the carboxyl groups of NaAl.

The IR spectra of serpentine with and without pre-treatment are shown in Figure 8c. For bare serpentine, adsorption bands at 3676 cm^{-1} were observed, indicating the stretching of -OH , which was also found for serpentine examined by other researchers [47,48]. The adsorption bands at 1085 cm^{-1} were attributed to the stretching vibration of Si-O . The out-of-plane bending vibration of Mg-O appeared at 563 cm^{-1} . Different from chlorite, there were no adsorption bands of silanol groups on the serpentine surface observed. After the pre-treatment of NaAl, there were new adsorption bands at 1629 cm^{-1} and 1424 cm^{-1} , which were attributed to the antisymmetric stretching vibration and symmetrical stretching vibration of -COO- , respectively. The observation of -COO- indicated that NaAl adsorbed on the surface of serpentine. The shifts (from 1608 cm^{-1} to 1629 cm^{-1} and from 1420 cm^{-1} to 1424 cm^{-1}) in the stretching bands of -COO- implied that NaAl chemically adsorbed on the surface of serpentine [35].



(a)

Figure 8. Cont.

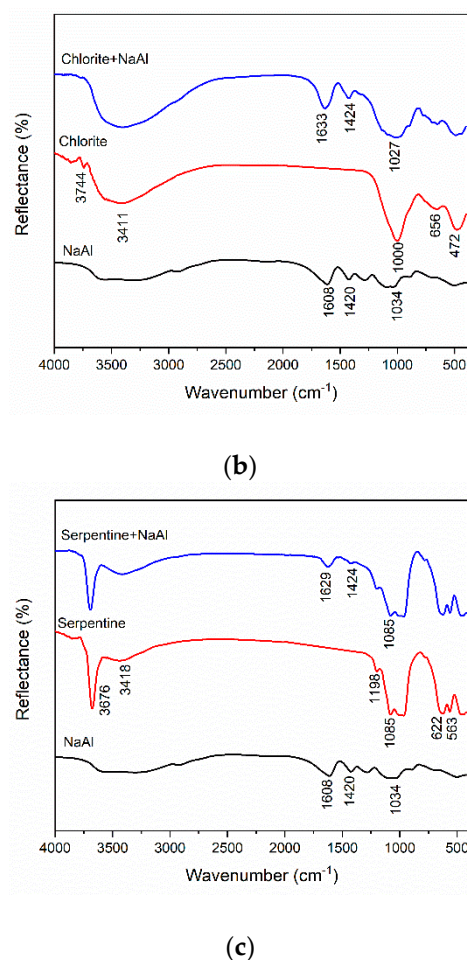


Figure 8. FTIR spectra of chalcopyrite (a), chlorite (b), and serpentine (c) with and without pre-treatment of NaAl.

3.6. Depression Mechanism of NaAl

According to the flotation, adsorption measurement, zeta potential, and FTIR results, the possible depression mechanism of NaAl on chlorite and serpentine minerals could be summarized as seen in Figure 9.

The depression effect of NaAl resulted from the complexation. It is known that NaAl could form a gel structure in the presence of divalent and multivalent cations such as (Ca^{2+} , Ni^{2+} , Cu^{2+} , Fe^{2+} , Al^{3+} , Mg^{2+}) by cross-linking of functional groups (such as $-\text{COO}-$, $\text{C}-\text{O}-\text{C}$, $-\text{OH}$) on the alginate chains of guluronate blocks [49]. Moreover, researchers found that carboxyl groups of alginate could interact with silanol groups of magnesium aluminum silicates by complexation [34,43]. Nevertheless, different surface properties of minerals affected the interaction between NaAl and the mineral surfaces, thereby swaying the adsorption capability and depression effect.

For bare chalcopyrite, its surface was rich in sulfur atoms [50], and the surface charge was highly negative with a zeta potential of -34.4 mV at pH 9. The electrostatic repulsion hindered the approach of the NaAl to chalcopyrite and blocked the interaction between metallic ions and NaAl. Therefore, there was no depression effect on chalcopyrite flotation.

However, for chlorite and serpentine, the situation was quite different. At pH 9, the surface zeta potential of bare chlorite was -17.1 mV. The electrostatic repulsion for chlorite was much smaller. Therefore, it was much easier for NaAl to approach chlorite surfaces. Chemical bonds on the end face of chlorite were broken to generate $\text{Si}-\text{OH}$ and $\text{Mg}-\text{OH}$ during the liberation process. The silanol groups interacted with the carboxyl groups of NaAl [43]. In addition, there were many metallic

ions on the staggered broken sides in which 1/3 of Mg^{2+} was replaced by Al^{3+} [14]. Functional groups (such as $-COO-$, $C-O-C$, $-OH$) of NaAl chelated with metallic ions (Al^{3+} , Fe^{2+} , Mg^{2+}) on chlorite surface. The chemical adsorption of NaAl on chlorite decreased its surface hydrophobicity and inhibited floatability; whereas, for serpentine, the depression mechanism was a little different than that of chlorite. The surface active groups of serpentine contain $Si-O-Si$, Si^{4+} , Mg^{2+} , and $-OH$ [51], where Mg^{2+} can be replaced by other metallic ions, such as Al^{3+} , Fe^{2+} , and Ni^{2+} . Functional groups (such as $-COO-$, $C-O-C$, $-OH$) of NaAl chelated with metallic ions (Al^{3+} , Fe^{2+} , Mg^{2+}) on the serpentine surface. According to the zeta potential measurement results, the adsorption of NaAl on serpentine reversed the mineral surface potential to -25.8 mV at pH 9, which generated strong electrical repulsion between serpentine particles and chalcopyrite particles, as well as chlorite particles. Moreover, since NaAl is a polymer, the adsorption of NaAl could also produce strong steric hindrance. Due to the electrical repulsion and steric hindrance, the serpentine was dispersed from chalcopyrite and chlorite surfaces, and further, the hetero-aggregation was prevented. Therefore, NaAl was able to depress two phyllosilicates simultaneously in the ternary mixture system.

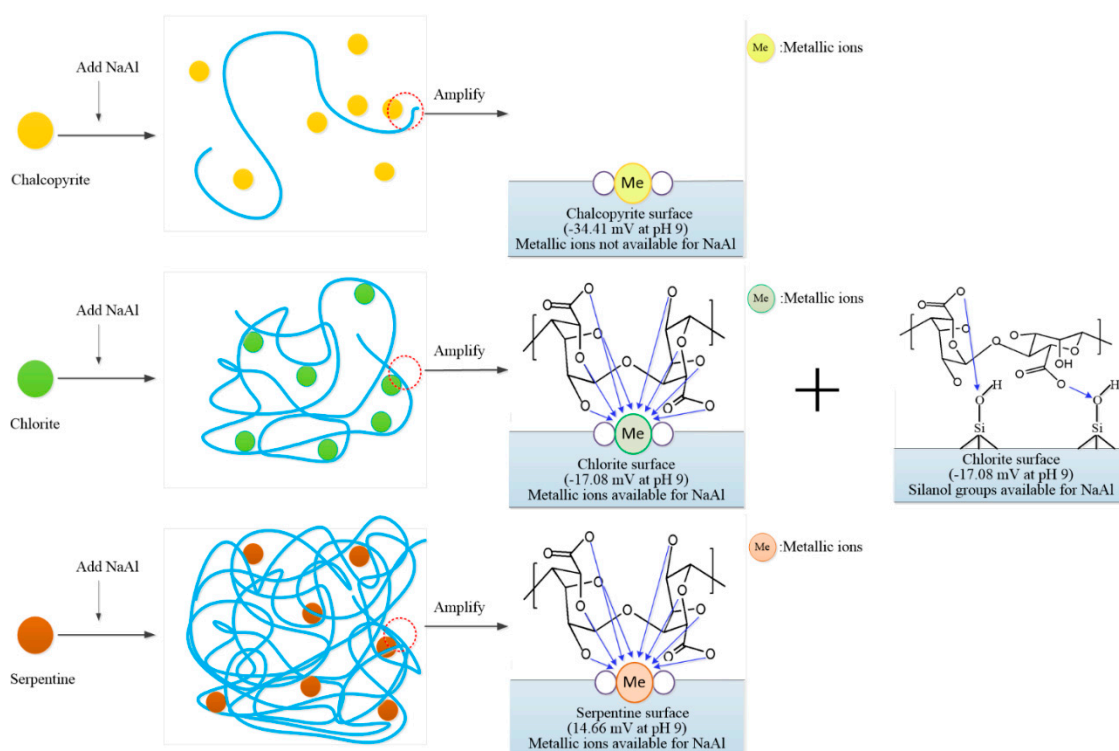


Figure 9. Schematic diagram of the adsorption behavior of NaAl on the minerals' surface.

4. Conclusions

Sodium alginate exhibited a simultaneous depression effect on chlorite and serpentine minerals in chalcopyrite flotation. With sodium alginate as a depressant, SAX as a collector, and MIBC as a frother, a good separation with concentrates Cu grade of 31% and Cu recovery of 90% could be achieved at pH 9 in the ternary mixture flotation. The flotation results demonstrated that NaAl simultaneously depressed chlorite and serpentine effectively. The selective depression on chlorite and serpentine was also validated by real ore flotation experiments. The adsorption measurements results (0.14 mg/m² saturated adsorption density of chlorite, 0.24 mg/m² of serpentine, and 0.02 mg/m² of chalcopyrite) gave the reason for the selective depression. Through analyzing the zeta potential and FTIR results, it was concluded that NaAl chemically adsorbed on the surface of chlorite and serpentine and further depressed their flotation at pH 9. NaAl can neither adsorb on the chalcopyrite surface nor interfere with its flotation behavior.

Author Contributions: Conceptualization, Q.S., G.P. and W.C.; methodology, G.P. and W.C.; validation, G.P. and W.C.; formal analysis, G.P.; investigation, G.P.; resources, G.Z. and Q.S.; writing—original draft preparation, G.P., Q.S. and W.C.; writing—review and editing, G.P. and Q.S.; supervision, G.Z. and Q.S.; project administration, G.Z. and Q.S.; funding acquisition, G.Z. and Q.S.

Funding: The authors acknowledge the support of the Central South University Graduate Research and Innovation Project (No. 2018zzts783), the Major State Basic Research Development Program of China (973 program) (2014CB643402), and the Key Laboratory of Hunan Province for Clean and Efficient Utilization of Strategic Calcium-containing Mineral Resources (No. 2018TP1002).

Conflicts of Interest: The authors declare no conflict of interest. The funders had no role in the design of the study; in the collection, analyses, or interpretation of data; in the writing of the manuscript, or in the decision to publish the results.

References

1. Suárez, S.; Nieto, F.; Velasco, F.; Martín, F.J. Serpentine and chlorite as effective Ni-Cu sinks during weathering of the Aguablanca sulphide deposit (SW Spain). TEM evidence for metal-retention mechanisms in sheet silicates. *Eur. J. Mineral.* **2011**, *23*, 179–196. [[CrossRef](#)]
2. Gur'yanov, V.A.; Prikhod'ko, V.S.; Perestoronin, A.N.; Petukhova, L.L.; Pototskii, Y.P.; Sobolev, L.P. New Type of Copper-Nickel Deposits in the Southeastern Aldan-Stanovoi Shield. *Dokl. Earth Sci.* **2009**, *425*, 363–366. [[CrossRef](#)]
3. Hamer, M.; Graham, R.C.; Amrhein, C.; Bozhilov, K.N. Dissolution of ripidolite (Mg, Fe-chlorite) in organic and inorganic acid solutions. *Soil Sci. Soc. Am. J.* **2003**, *67*, 654–661. [[CrossRef](#)]
4. Palandri, J.L.; Reed, M.H. Geochemical models of metasomatism in ultramafic systems: Serpentinization, rodingitization, and sea floor carbonate chimney precipitation 1. *Geochim. Cosmochim. Acta* **2004**, *68*, 1115–1133. [[CrossRef](#)]
5. Austrheim, H.; Prestvik, T. Rodingitization and hydration of the oceanic lithosphere as developed in the Leka ophiolite, north-central Norway. *Lithos* **2008**, *104*, 177–198. [[CrossRef](#)]
6. Zhang, W.; Zhu, G.C.; Wu, Y.Z. The enrichment mechanism of PGE and characteristic of MSZ in HW mining area in Great Dyke Zimbabwe. *Adv. Mater. Res.* **2013**, *616*, 90–95. [[CrossRef](#)]
7. Parman, S.W.; Grove, T.L. Petrology and geochemistry of Barberton komatiites and basaltic komatiites: Evidence of Archean fore-arc magmatism. *Dev. Precambrian Geol.* **2004**, *13*, 539–565.
8. Bobicki, E.R.; Liu, Q.; Xu, Z. Effect of microwave pre-treatment on ultramafic nickel ore slurry rheology. *Miner. Eng.* **2014**, *61*, 97–104. [[CrossRef](#)]
9. Tan, H.; Skinner, W.; Addai-Mensah, J. Influence of fluorite on the isothermal leaching and rheological behaviours of chlorite mineral pulps at low pH. *Int. J. Miner. Process.* **2013**, *123*, 1–8. [[CrossRef](#)]
10. Chen, X.; Peng, Y. Managing clay minerals in froth flotation—A critical review. *Miner. Process. Extr. Metall. Rev.* **2018**, *39*, 289–307. [[CrossRef](#)]
11. Feng, B.; Lu, Y.; Feng, Q.; Zhang, M.; Gu, Y. Talc-serpentine interactions and implications for talc depression. *Miner. Eng.* **2012**, *32*, 68–73. [[CrossRef](#)]
12. Jin, S.; Shi, Q.; Li, Q.; Ou, L.; Ouyang, K. Effect of calcium ionic concentrations on the adsorption of carboxymethyl cellulose onto talc surface: Flotation, adsorption and AFM imaging study. *Powder Technol.* **2018**, *331*, 155–161. [[CrossRef](#)]
13. Silvester, E.J.; Bruckard, W.J.; Woodcock, J.T. Surface and chemical properties of chlorite in relation to its flotation and depression. *Miner. Process. Extr. Metall.* **2011**, *120*, 65–70. [[CrossRef](#)]
14. Zheng, G.; Liu, L.; Liu, J.; Wang, Y.; Cao, Y. Study of chlorite flotation and its influencing factors. *Procedia Earth Planet. Sci.* **2009**, *1*, 830–837.
15. Fornasiero, D.; Ralston, J. Cu(II) and Ni(II) activation in the flotation of quartz, lizardite and chlorite. *Int. J. Miner. Process.* **2005**, *76*, 75–81. [[CrossRef](#)]
16. Alvarez-Silva, M.; Uribe-Salas, A.; Mirnezami, M.; Finch, J.A. The point of zero charge of phyllosilicate minerals using the Mular–Roberts titration technique. *Miner. Eng.* **2010**, *23*, 383–389. [[CrossRef](#)]
17. Bo, F.; Lu, Y.; Feng, Q.; Peng, D.; Na, L.U.O. Mechanisms of surface charge development of serpentine mineral. *Trans. Nonferrous Met. Soc. China* **2013**, *23*, 1123–1128.
18. Feng, B.; Feng, Q.; Lu, Y. The effect of lizardite surface characteristics on pyrite flotation. *Appl. Surf. Sci.* **2012**, *259*, 153–158. [[CrossRef](#)]

19. Peng, Y.; Bradshaw, D. Mechanisms for the improved flotation of ultrafine pentlandite and its separation from lizardite in saline water. *Miner. Eng.* **2012**, *36*, 284–290. [[CrossRef](#)]
20. Feng, B.; Feng, Q.; Lu, Y. A novel method to limit the detrimental effect of serpentine on the flotation of pentlandite. *Int. J. Miner. Process.* **2012**, *114*, 11–13. [[CrossRef](#)]
21. Jin, S.; Shi, Q.; Feng, Q.; Zhang, G.; Chang, Z. The role of calcium and carbonate ions in the separation of pyrite and talc. *Miner. Eng.* **2018**, *119*, 205–211. [[CrossRef](#)]
22. Feng, B.; Peng, J.; Guo, W.; Zhang, W.; Ai, G.; Wang, H. The effect of changes in pH on the depression of talc by chitosan and the associated mechanisms. *Powder Technol.* **2018**, *325*, 58–63. [[CrossRef](#)]
23. Zhao, K.; Gu, G.; Wang, C.; Rao, X.; Wang, X.; Xiong, X. The effect of a new polysaccharide on the depression of talc and the flotation of a nickel–copper sulfide ore. *Miner. Eng.* **2015**, *77*, 99–106. [[CrossRef](#)]
24. Liu, G.; Feng, Q.; Ou, L.; Lu, Y.; Zhang, G. Adsorption of polysaccharide onto talc. *Miner. Eng.* **2006**, *19*, 147–153. [[CrossRef](#)]
25. Ma, X.; Pawlik, M. The effect of lignosulfonates on the floatability of talc. *Int. J. Miner. Process.* **2007**, *83*, 19–27. [[CrossRef](#)]
26. Lee, K.Y.; Mooney, D.J. Alginate: Properties and biomedical applications. *Prog. Polym. Sci.* **2012**, *37*, 106–126. [[CrossRef](#)]
27. Daemi, H.; Barikani, M. Synthesis and characterization of calcium alginate nanoparticles, sodium homopolymannuronate salt and its calcium nanoparticles. *Sci. Iran.* **2012**, *19*, 2023–2028. [[CrossRef](#)]
28. Pawar, S.N.; Edgar, K.J. Alginate derivatization: A review of chemistry, properties and applications. *Biomaterials* **2012**, *33*, 3279–3305. [[CrossRef](#)] [[PubMed](#)]
29. Thakur, S.; Sharma, B.; Verma, A.; Chaudhary, J.; Tamulevicius, S.; Thakur, V.K. Recent progress in sodium alginate based sustainable hydrogels for environmental applications. *J. Clean. Prod.* **2018**, *198*, 143–159. [[CrossRef](#)]
30. Gombotz, W.R.; Wee, S.F. Protein release from alginate matrices. *Adv. Drug Deliv. Rev.* **2012**, *64*, 194–205. [[CrossRef](#)]
31. Topuz, F.; Henke, A.; Richtering, W.; Groll, J. Magnesium ions and alginate do form hydrogels: A rheological study. *Soft Matter* **2012**, *8*, 4877–4881. [[CrossRef](#)]
32. Jana, S.; Gandhi, A.; Sheet, S.; Sen, K.K. Metal ion-induced alginate–locust bean gum IPN microspheres for sustained oral delivery of aceclofenac. *Int. J. Biol. Macromol.* **2015**, *72*, 47–53. [[CrossRef](#)]
33. Tønnesen, H.H.; Karlsen, J. Alginate in drug delivery systems. *Drug Dev. Ind. Pharm.* **2002**, *28*, 621–630. [[CrossRef](#)]
34. Pongjanyakul, T.; Priprem, A.; Puttipipatkachorn, S. Investigation of novel alginate–magnesium aluminum silicate microcomposite films for modified-release tablets. *J. Control. Release* **2005**, *107*, 343–356. [[CrossRef](#)] [[PubMed](#)]
35. Chen, W.; Feng, Q.; Zhang, G.; Yang, Q.; Zhang, C. The effect of sodium alginate on the flotation separation of scheelite from calcite and fluorite. *Miner. Eng.* **2017**, *113*, 1–7. [[CrossRef](#)]
36. Chen, Z.; Gu, G.; Li, S.; Wang, C.; Zhu, R. The Effect of Seaweed Glue in the Separation of Copper–Molybdenum Sulphide Ore by Flotation. *Minerals* **2018**, *8*, 41. [[CrossRef](#)]
37. Wellham, E.J.; Elber, L.; Yan, D.S. The role of carboxy methyl cellulose in the flotation of a nickel sulphide transition ore. *Miner. Eng.* **1992**, *5*, 381–395. [[CrossRef](#)]
38. Duarte, A.C.P.; Grano, S.R. Mechanism for the recovery of silicate gangue minerals in the flotation of ultrafine sphalerite. *Miner. Eng.* **2007**, *20*, 766–775. [[CrossRef](#)]
39. Miller, J.D.; Li, J.; Davidtz, J.C.; Vos, F. A review of pyrrhotite flotation chemistry in the processing of PGM ores. *Miner. Eng.* **2005**, *18*, 855–865. [[CrossRef](#)]
40. Zouboulis, A.I.; Kydros, K.A.; Matis, K.A. Adsorbing flotation of copper hydroxide precipitates by pyrite fines. *Sep. Sci. Technol.* **1992**, *27*, 2143–2155. [[CrossRef](#)]
41. Bellamy, L.J. The infrared spectra of complex molecules. In *The Infrared Spectra of Complex Molecules*; Springer Science & Business Media: Berlin, Germany, 2013; pp. 183–202, ISBN 0412138506.
42. Rath, R.K.; Subramanian, S.; Pradeep, T. Surface chemical studies on pyrite in the presence of polysaccharide-based flotation depressants. *J. Colloid Interface Sci.* **2000**, *229*, 82–91. [[CrossRef](#)]
43. Puttipipatkachorn, S.; Pongjanyakul, T.; Priprem, A. Molecular interaction in alginate beads reinforced with sodium starch glycolate or magnesium aluminum silicate, and their physical characteristics. *Int. J. Pharm.* **2005**, *293*, 51–62. [[CrossRef](#)]

44. Sondi, I.; Milat, O.; Pravdić, V. Electrokinetic potentials of clay surfaces modified by polymers. *J. Colloid Interface Sci.* **1997**, *189*, 66–73. [[CrossRef](#)]
45. Sondi, I.; Pravdić, V. Electrokinetics of natural and mechanically modified ripidolite and beidellite clays. *J. Colloid Interface Sci.* **1996**, *181*, 463–469. [[CrossRef](#)]
46. Sondi, I.; Pravdic, V. The colloid and surface chemistry of clays in natural waters. *Croat. Chem. Acta* **1998**, *71*, 1061–1074.
47. Zaikowski, A. Infrared spectra of the Orgueil (C-1) chondrite and serpentine minerals. *Geochim. Cosmochim. Acta* **1979**, *43*, 943–945. [[CrossRef](#)]
48. Heller-Kallai, L.; Yariv, S.; Gross, S. Hydroxyl-stretching frequencies of serpentine minerals. *Mineral. Mag.* **1975**, *40*, 197–200. [[CrossRef](#)]
49. Andersen, T.; Auk-Emblem, P.; Dornish, M. 3D Cell Culture in Alginate Hydrogels. *Microarrays* **2015**, *4*, 133–161. [[CrossRef](#)] [[PubMed](#)]
50. Wen, S.M.; Deng, J.S.; Xian, Y.J.; Dan, L. Theory analysis and vestigial information of surface relaxation of natural chalcopyrite mineral crystal. *Trans. Nonferrous Met. Soc. China* **2013**, *23*, 796–803. [[CrossRef](#)]
51. Li, X.; Wang, L.; Lu, A. A discussion on activation mechanism of atom groups in serpentine. *ACTA Petrol. Mineral.* **2003**, *22*, 386–390.



© 2019 by the authors. Licensee MDPI, Basel, Switzerland. This article is an open access article distributed under the terms and conditions of the Creative Commons Attribution (CC BY) license (<http://creativecommons.org/licenses/by/4.0/>).